

## Electronic Supporting Information

### **Dynamic nanoconfinement strategy towards self-healing soft electronics with superstretchability, ultrahigh strength and reliably high conductivity**

Jun-Peng Wang,<sup>a,b\*</sup> Chuhan Fu,<sup>c</sup> Zehua Wu,<sup>d</sup> Hao Lan,<sup>a,b</sup> Siwen Cui,<sup>e\*</sup> and Tao Qi<sup>a\*</sup>

<sup>a</sup> Jiangxi Province Key Laboratory of Cleaner Production of Rare Earths, Ganjiang Innovation Academy, Chinese Academy of Sciences, Ganzhou 341000, China

<sup>b</sup> Institute of Process Engineering, Chinese Academy of Sciences, Beijing 100190, China

<sup>c</sup> School of Rare earths, University of Science and Technology of China, Hefei 230026, China

<sup>d</sup> Key Laboratory of Chemical lasers, Dalian Institute of Chemical Physics, Chinese Academy of Sciences, Dalian 116024, China

<sup>e</sup> Center for Advanced Materials Research, Zhongyuan University of Technology, Zhengzhou 450007, China.

\*Corresponding author E-mails: wangjunpeng@gia.cas.cn; cuiuwen@zut.edu.cn; tqi@gia.cas.cn

Keywords: bioinspired nanoconfinement, self-healing electronics, superstretchability, ultrahigh strength, reliably high conductivity

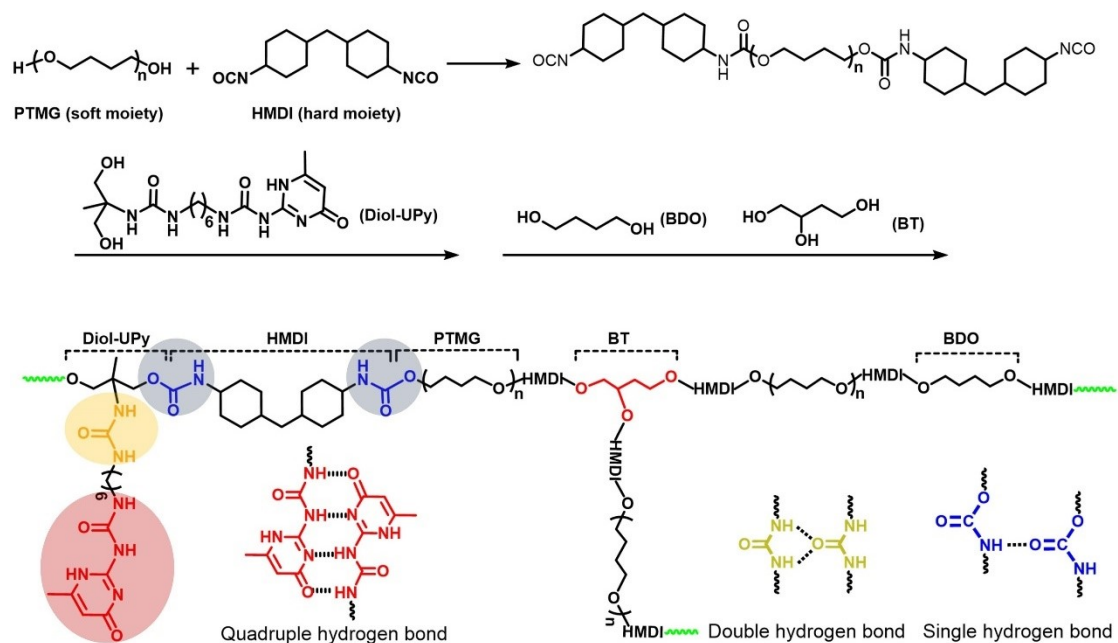


**Figure S1.** The synthesis route of TSPU polymer. In the final self-healing polymer matrix, there existed hierarchical (single, double, quadruple) hydrogen bonding interactions, which induced the aggregation of H-bonds from hard moieties forming nanoconfined phase.

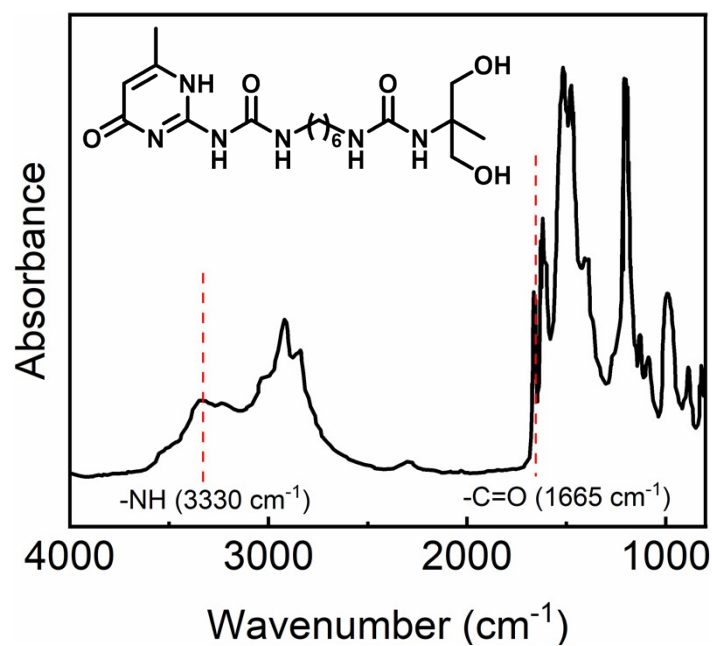


**Figure S2.** The FTIR spectrum of Diol-UPy.

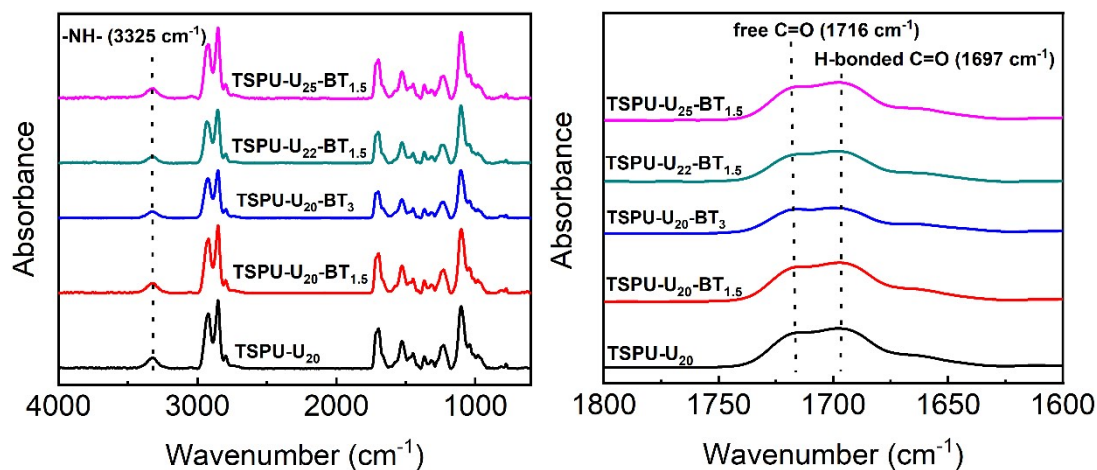


**Figure S3.** FTIR spectra of TSPU elastomers. The absorption peaks at  $3325\text{ cm}^{-1}$ ,  $1716\text{ cm}^{-1}$  and  $1697\text{ cm}^{-1}$  were attributed to the absorbance of  $\text{-NH-}$ , free  $\text{C=O}$  and H-bonded  $\text{C=O}$ , respectively.

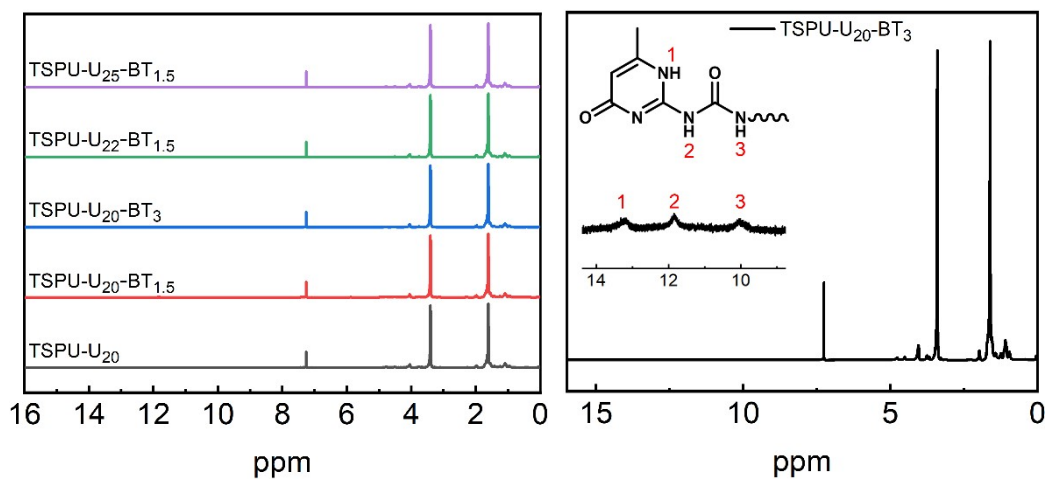


**Figure S4.**  $^1\text{H}$ NMR spectra of TSPU elastomers. The chemical shifts at  $13.21\text{ ppm}$ ,  $11.85\text{ ppm}$ , and  $10.06\text{ ppm}$  demonstrated the existence of UPy groups.

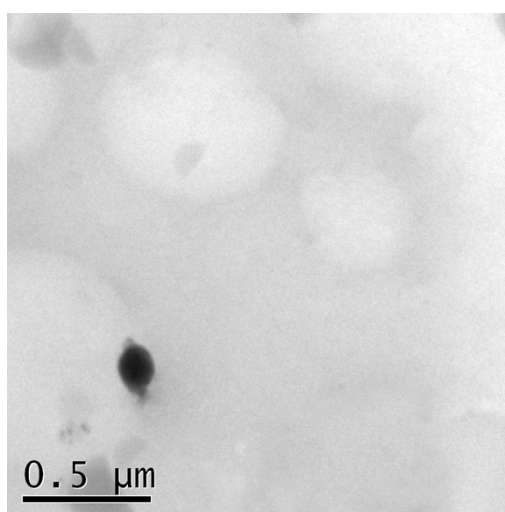


**Figure S5.** Characterization of TSPU- $\text{U}_{25}\text{-BT}_{1.5}$  polymer with TEM.



**Figure S6.** Optical photographs of TSPU elastomer at 0% (left) and 2000% (right) strains.

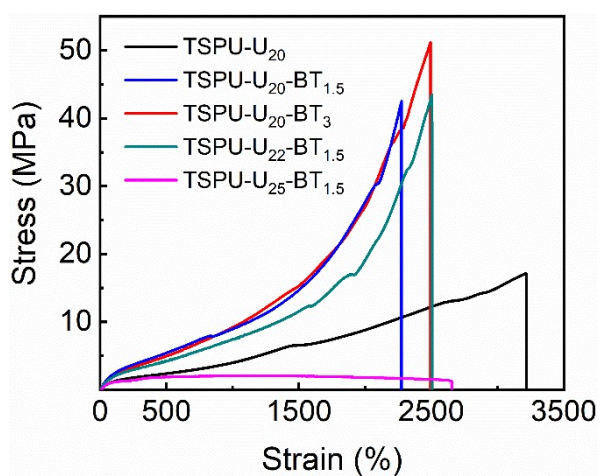


**Figure S7.** The engineering stress-strain curves of as-synthesized TSPU elastomers.



**Figure S8.** The weights of dumbbell and TSPU sample used to lift up dumbbell.

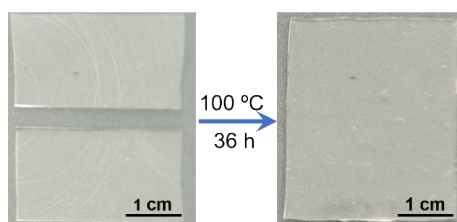


**Figure S9.** The cut-off sample was self-healed after handled at 100 °C for 36 h.

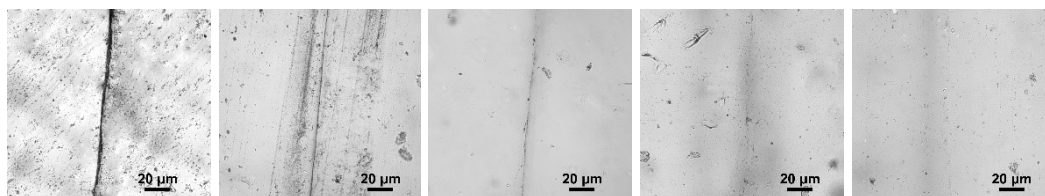


**Figure S10.** The microscopy images of self-healing process for reattached two cut-off pieces at 100 °C for 0 h, 4 h, 12 h, 24 h, 36 h (from left to right).

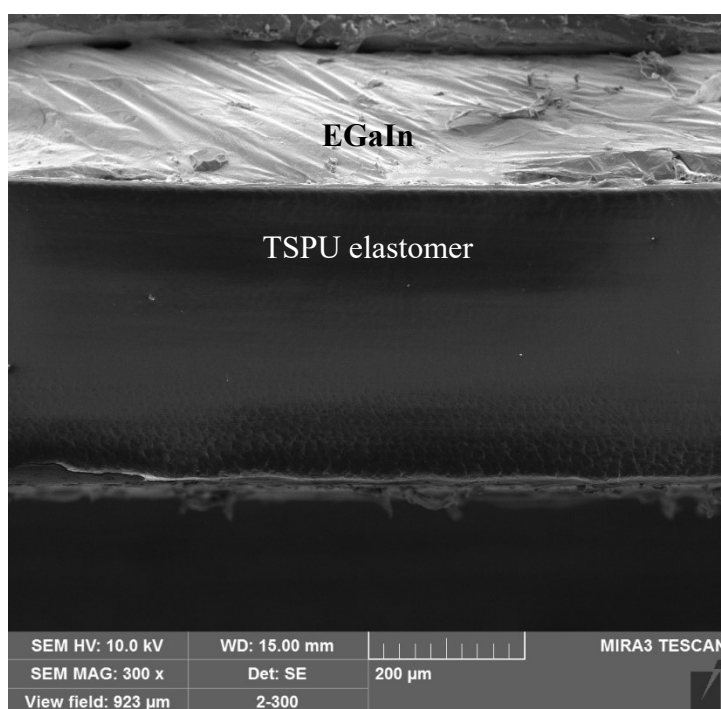


**Figure S11.** Cross-profile image of electrode characterized by SEM. It is shown that EGaIn liquid metal spreads on TSPU elastomer and the thickness of EGaIn is ca. 170 μm.

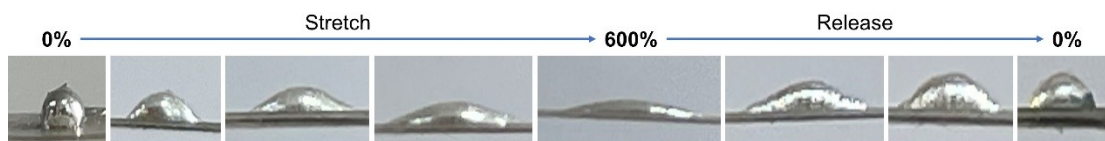


**Figure S12.** (a) Photographs of EGaIn droplet illustrating a well surface reconciliation on a TSPU-U<sub>20</sub>-BT<sub>3</sub> specimen during stretching and releasing process.

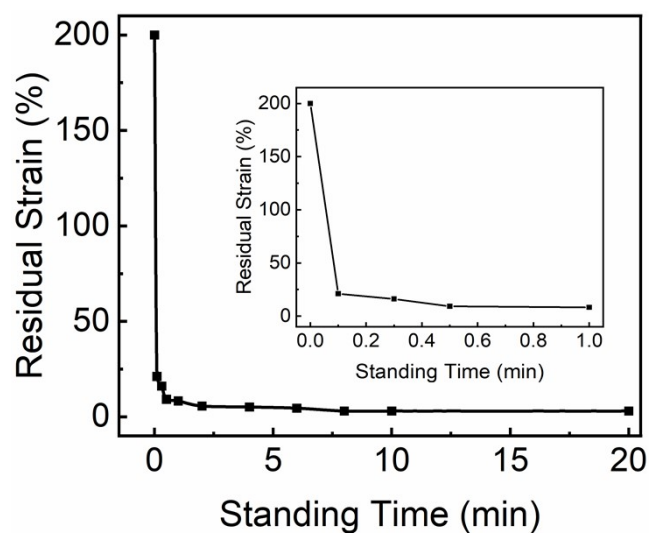


**Figure S13.** The dependence of residual strain on standing time of relaxed TSPU after being stretched to 300% strain.

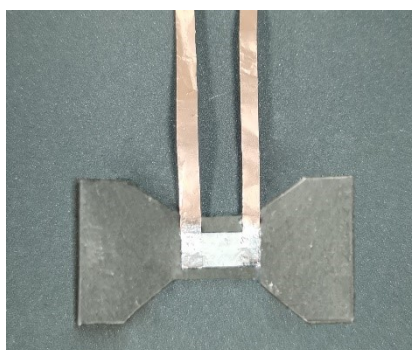


**Figure S14.** Soft electrode used for measuring its conductivity.

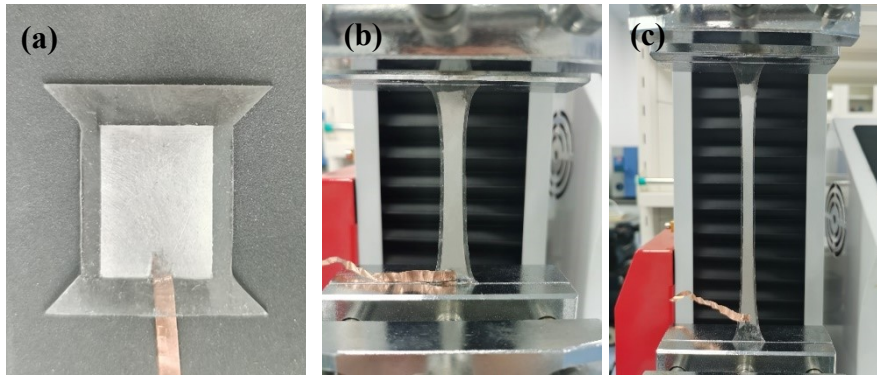


**Figure S15.** The photography images of supertough self-healing triboelectric nanogenerator (TS-TENG, working area: 3 cm × 2 cm) (a) and its tensile states at 500% (b) and 900% (c) strains.

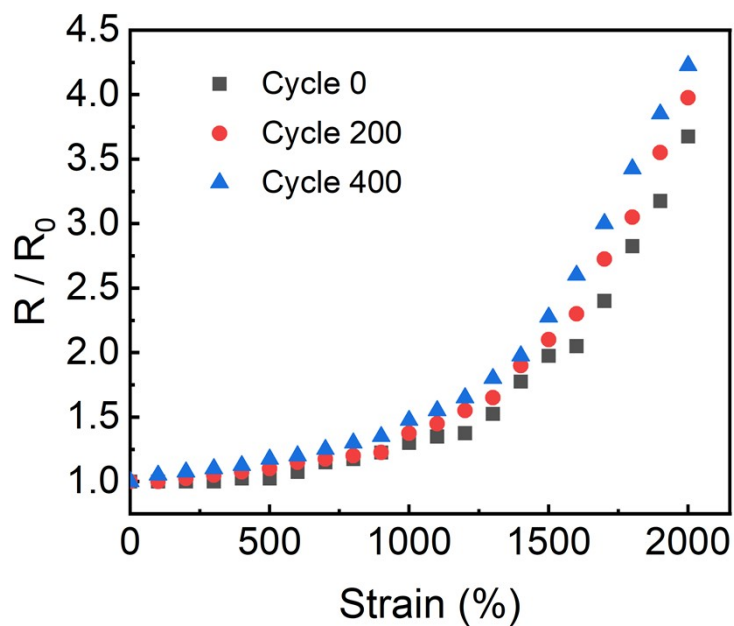


**Figure S16.** The dependence of  $R / R_0$  on strain of healed electrode after varied stretch-release cycles. One stretch-release cycle is referred to the electrode stretched to 100% and then released.

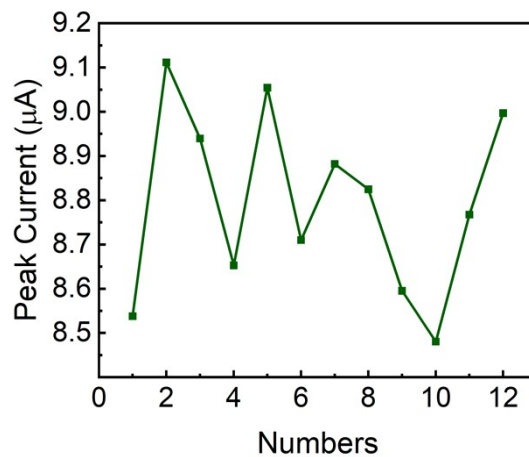


**Figure S17.** The variation of peak short circuit current of TS-TENG versus testing numbers. The standard

Entry	Electrodes	Strain (%)	Stress (MPa)	R/R <sub>0</sub>	Healing efficiency (%)	Ref.
A	DMSO/PEDOT:PSS	32	11.5	9.5@40%	No	1
B	P(AAm-co-HEMA)/PANI	90	17.5	1.8@70%	No	2
C	F-PNIPAAm/PANI	187	0.042	5.5@120%	No	3
D	Ionic conductive cellulose hydrogel (CCH)	220	2	2.62@220%	No	4
E	P(AN/AANa)	425	23.17	3.5@425%	No	5
F	PVA <sub>2</sub> PEI <sub>1-75</sub>	500	0.6	14.5@460%	No	6
G	PADL <sub>3</sub> hydrogel	500	0.052	31@500%	93	7
H	PEDOT:PSS-PAAm organogels	525	0.03	17@300%	No	8
I	PVA-1% CNF	625	1.4	6.76@400%	No	9
J	PAA-rGO hydrogel	630	0.4	5.25@500%	75	10
K	SACP film	700	1.2	81@400%	No	11
L	PVA/GE/GL/NaCl gels	715	1.04	6@600%	No	12
M	HPC/PVA <sub>16%</sub> hydrogel	800	1.3	9@400%	No	13
N	PAA/PANI/glycerol/Fe <sup>3+</sup>	991	0.0357	31@275%	90.8	14
O	GN-CNF@PVA hydrogel	1000	0.0037	21@500%	98.9	15
P	MXene/PVA/PAAm	1000	0.035	76@350%	85	16
Q	PAAm-oxCNTs	1044	0.71	21@700%	No	17
R	Cel <sub>14</sub> /PAA-Fe <sub>2.50</sub> <sup>3+</sup> hydrogel	1755	0.1	64@1100%	No	18
S	VP/PP/ZP/Al <sup>3+</sup> hydrogels	1769	0.46	23.5@700%	91.8	19
T	PDMS-MPU <sub>0.4</sub> -IU <sub>0.6</sub>	1842	1.5	6@500%	78	20
U	HPAAN/PDA	1845	0.438	1.3@200%	49	21
V	AFPs <sub>50</sub> .PAM/PVA <sub>0.5</sub>	2358	0.058	97@1000%	No	22
W	MGP	2700	0.3	41@2700%	No	23
X	LPBP hydrogel	2850	0.2	18@500%	98.6	24
Y	DAE-3	5100	1.9	301@100%	86	25
Z	This work	~2500	~50	3.63@2000%	82.9	

deviation is 0.21  $\mu$ A.

**Table S1** Comparison of comprehensive performance of electrode herein to that of previously reported stretchable electrodes.



## References

1. H. He, L. Zhang, S. Yue, S. Yu, J. Wei and J. Ouyang, *Macromolecules*, 2021, **54**, 1234.
2. Z. Wang, J. Chen, Y. Cong, H. Zhang, T. Xu, L. Nie and J. Fu, *Chem. Mater.*, 2018, **30**, 8062.
3. Z. Wang, H. Zhou, W. Chen, Q. Li, B. Yan, X. Jin, A. Ma, H. Liu and W. Zhao, *ACS Appl. Mater. Interfaces*, 2018, **10**.
4. Y. Wang, L. Zhang and A. Lu, *ACS Appl. Mater. Interfaces*, 2019, **11**.
5. S. Cai, B. Niu, X. Ma, S. Wan and X. He, *Chem. Eng. J.*, 2022, **430**, 132957.
6. C. Wang, K. Hu, C. Zhao, Y. Zou, Y. Liu, X. Qu, D. Jiang, Z. Li, M. R. Zhang and Z. Li, *Small*, 2020, **16**.
7. L. Jiang, J. Liu, S. He, A. Liu, J. Zhang, H. Xu and W. Shao, *Chem. Eng. J.*, 2022, **430**, 132653.
8. Y. Y. Lee, H. Y. Kang, S. H. Gwon, G. M. Choi, S. M. Lim, J. Y. Sun and Y. C. Joo, *Adv. Mater.*, 2016, **28**.
9. Y. Ye, Y. Zhang, Y. Chen, X. Han and F. Jiang, *Adv. Funct. Mater.*, 2020, **30**, 2003430.
10. X. Jing, H.-Y. Mi, X.-F. Peng and L.-S. Turng, *Carbon*, 2018, **136**, 63.
11. P. Tan, H. Wang, F. Xiao, X. Lu, W. Shang, X. Deng, H. Song, Z. Xu, J. Cao, T. Gan, B. Wang and X. Zhou, *Nat. Commun.*, 2022, **13**.
12. H. Chen, X. Ren and G. Gao, *ACS Appl. Mater. Interfaces*, 2019, **11**.
13. Y. Zhou, C. Wan, Y. Yang, H. Yang, S. Wang, Z. Dai, K. Ji, H. Jiang, X. Chen and Y. Long, *Adv. Funct. Mater.*, 2019, **29**, 1806220.
14. G. Ge, Y. Lu, X. Qu, W. Zhao, Y. Ren, W. Wang, Q. Wang, W. Huang and X. Dong, *ACS Nano*, 2020, **14**.
15. C. Zheng, Y. Yue, L. Gan, X. Xu, C. Mei and J. Han, *Nanomaterials*, 2019, **9**, 937.
16. H. Liao, X. Guo, P. Wan and G. Yu, *Adv. Funct. Mater.*, 2019, **29**, 1904507.
17. X. Sun, Z. Qin, L. Ye, H. Zhang, Q. Yu, X. Wu, J. Li and F. Yao, *Chem. Eng. J.*, 2020, **382**, 122832.
18. F. Lu, Y. Wang, C. Wang, S. Kuga, Y. Huang and M. Wu, *ACS Sustain. Chem. Eng.*, 2020, **8**, 3427.
19. E. Feng, J. Li, G. Zheng, X. Li, J. Wei, Z. Wu, X. Ma and Z. Yang, *Chem. Eng. J.*, 2022, **432**, 134406.

20. J. Kang, D. Son, G. N. Wang, Y. Liu, J. Lopez, Y. Kim, J. Y. Oh, T. Katsumata, J. Mun, Y. Lee, L. Jin, J. B. Tok and Z. Bao, *Adv. Mater.*, 2018, **30**.
21. Z. Gao, L. Kong, R. Jin, X. Liu, W. Hu and G. Gao, *J. Mater. Chem. C*, 2020, **8**, 11119.
22. Y. Wang, Y. Xia, P. Xiang, Y. Dai, Y. Gao, H. Xu, J. Yu, G. Gao and K. Chen, *Chem. Eng. J.*, 2022, **428**, 131171.
23. H. Sun, Y. Zhao, C. Wang, K. Zhou, C. Yan, G. Zheng, J. Huang, K. Dai, C. Liu and C. Shen, *Nano Energy*, 2020, **76**, 105035.
24. M. Wang, X. Feng, X. Wang, S. Hu, C. Zhang and H. Qi, *J. Mater. Chem. A*, 2021, **9**, 24539.
25. Z. Xu, L. Chen, L. Lu, R. Du, W. Ma, Y. Cai, X. An, H. Wu, Q. Luo, Q. Xu, Q. Zhang and X. Jia, *Adv. Funct. Mater.*, 2020, **31**, 2006432.